Research Square

Preprints are preliminary reports that have not undergone peer review.
They should not be considered conclusive, used to inform clinical practice,
or referenced by the media as validated information.

KRIT1 Haploinsufficiency Alters Hepatic Lipid/Sphingolipid Metabolism: Exacerbation by a High Fructose Diet

Raffaella Mastrocola

raffaella.mastrocola@unito.it

University of Turin Department of Clinical and Biological Science: Universita Degli Studi di Torino Dipartimento di Scienze Cliniche e Biologiche https://orcid.org/0000-0002-0104-6129

Giada Corsini

University of Turin Department of Clinical and Biological Science: Universita Degli Studi di Torino Dipartimento di Scienze Cliniche e Biologiche

Claudia Fornelli

University of Turin Department of Clinical and Biological Science: Universita Degli Studi di Torino Dipartimento di Scienze Cliniche e Biologiche

Federica Dal Bello

University of Turin Department of Molecular Biotechnology and Health Sciences: Universita degli Studi di Torino Dipartimento di Biotecnologie Molecolari e Scienze per la Salute

Andrea Perrelli

Department of Pharmacology and Physiology, University of Rochester Medical Center

Chiara Ferraris

University of Turin Department of Clinical and Biological Science: Universita Degli Studi di Torino Dipartimento di Scienze Cliniche e Biologiche

Luca Goitre

University of Turin Department of Clinical and Biological Science: Universita Degli Studi di Torino Dipartimento di Scienze Cliniche e Biologiche

Saverio Francesco Retta

University of Turin Department of Clinical and Biological Science: Universita Degli Studi di Torino Dipartimento di Scienze Cliniche e Biologiche

---

Research Article

Keywords: KRIT1/CCM1, hepatic sphingolipid dysmetabolism, liver inflammation and fibrosis, advanced glycation endproducts (AGEs), sphingosine-1-phosphate (S1P), S1P/RhoA/ROCK/YAP pathway.

Posted Date: November 17th, 2026

DOI: https://doi.org/10.21203/rs.3.rs-11455639/v1

License: This work is licensed under a Creative Commons Attribution 4.0 International License.
Read Full License

KRIT1 Haploinsufficiency Alters Hepatic Lipid/Sphingolipid Metabolism: Exacerbation by a High Fructose Diet

Raffaella Mastrocola[1,2,*], Giada Corsini[1], Claudia Fornelli[1,2], Federica Dal Bello[3], Andrea Perrelli[2,4], Chiara Ferraris[1,2], Luca Goitre[1,2], Saverio Francesco Retta[1,2,]

[1]Department of Clinical and Biological Sciences, University of Torino, Orbassano (TO), Italy

[2]CCM Italia Research Network, National Coordination Center at the Department of Clinical and Biological Sciences, University of Torino, Orbassano (TO), Italy

[3]Department of Molecular Biotechnology and Health Sciences, University of Torino, Torino, Italy

[4]Department of Pharmacology and Physiology, University of Rochester Medical Center, Rochester, NY, USA

***Corresponding author:**

Prof. Raffaella Mastrocola
University of Turin
Dept. of Clinical and Biological Sciences
Corso Raffaello 30 - 10125 Torino
raffaella.mastrocola@unito.it

Abstract

Background. Loss-of-function mutations in KRIT1 gene cause familial cerebral cavernous malformations (CCM), a neurovascular disorder characterized by fragile, leaky capillaries in brain. Beyond its role in vascular integrity, KRIT1 also regulates redox and metabolic signaling, yet its systemic impact remains poorly understood. Given its involvement in mevalonate pathway signaling and modulation of the RhoA/ROCK/YAP axis, we investigated whether KRIT1 haploinsufficiency alters hepatic lipid and sphingolipid metabolism and how dietary stress may exacerbate these effects.

Methods. Wild-type (WT) and KRIT1 heterozygous (HZ) mice were fed either a control or high-fructose (60%) diet for 22 weeks. Hepatic glycative stress, S1P pathway components, inflammatory and fibrotic markers, and RhoA/ROCK/YAP signaling were assessed via molecular, histological, and biochemical analyses. In vitro, KRIT1-silenced and KRIT1-overexpressing fibroblasts were used to validate KRIT1-dependent regulation of lipid and S1P metabolism.

Results. KRIT1 haploinsufficiency induced hepatic steatosis, increased *de novo* lipogenesis, S1P synthesis and S1PR1/S1PR3 expression, alongside AGE/RAGE axis, inflammatory and fibrotic markers. A high-fructose diet amplified these changes, enhancing activation of the S1P/RhoA/ROCK/YAP axis and liver pathology. *In vitro* studies confirmed direct involvement of KRIT1 in lipid homeostasis and pro-inflammatory signaling.

Conclusion. Our findings reveal a novel systemic function of KRIT1 in maintaining hepatic lipid and sphingolipid balance through the S1P/RhoA/ROCK/YAP pathway. Dietary fructose exacerbates KRIT1-dependent metabolic dysregulation, providing new insights into gene–environment interactions that may contribute to CCM progression and extracerebral comorbidities. These results broaden the pathological framework of KRIT1 beyond the cerebral endothelium and highlight the metabolic context as a key modifier of disease expression.

Keywords

KRIT1/CCM1; hepatic sphingolipid dysmetabolism; liver inflammation and fibrosis; advanced glycation endproducts (AGEs); sphingosine-1-phosphate (S1P); S1P/RhoA/ROCK/YAP pathway.

Introduction

KRIT1 (Krev interaction trapped-1) was originally identified as a gene encoding a binding protein of the small GTPase Rap1, a key regulator of cell adhesion and proliferation [1, 2], and subsequently shown to be implicated in the pathogenesis of cerebral cavernous malformation (CCM) disease, a cerebrovascular disorder consisting of clusters of dilated capillaries prone to leakage and hemorrhage [3, 4]. CCM occurs in both sporadic (80%) and familial (20%) forms, affects approximately 0.5% of the population, and can remain asymptomatic or present with headaches, seizures, focal neurological deficits, and intracerebral hemorrhage [5, 6]. Loss-of-function mutations in KRIT1 account for at least 50% of familial CCM cases [7]. These mutations impair endothelial cell-cell junction stability and blood-brain barrier integrity through overactivation of the small GTPase RhoA and its downstream effector Rho-associated kinase (ROCK) [8-10], as well as through additional pathogenic mechanisms involving altered redox homeostasis and signalling [11]. Among these mechanisms, dysregulation of the RhoA/ROCK mechanotransduction pathway has emerged as a key driver of CCM pathogenesis and a promising therapeutic target [10, 12, 13]. Although surgical resection remains the only established treatment for symptomatic lesions, pharmacological inhibition of this pathway, including the use of statins and fasudil, has shown efficacy in reducing lesion development in experimental CCM models [14-17].

Despite these advances, the molecular link between KRIT1 loss-of-function and RhoA/ROCK activation remains incompletely understood, as multiple direct and indirect regulatory mechanisms have been proposed [14]. Conversely, growing evidence suggests that many of the pleiotropic effects associated with KRIT1 deficiency may originate from its role in the regulation of redox homeostasis and signalling. Indeed, KRIT1 influences several redox-sensitive pathways, including RhoA/ROCK, FOXO1, mTORC1 and NRF2 signalling, as well as oxy-inflammatory responses [11, 18-21].

Beyond providing an alternative mechanistic framework for CCM pathogenesis, the recognition that KRIT1 deficiency induces widespread redox-dependent alterations, including impaired cell adhesion, cytoskeletal remodelling and increased susceptibility to oxy-inflammatory stress, has also helped explain the incomplete penetrance and highly variable clinical expressivity of the disease [22-24]. Furthermore, it offers a unifying explanation for the beneficial effects reported for several pharmacological approaches tested in experimental CCM models, including statins, fasudil, sulindac, vitamin D, tempol and rapamycin [11, 25-30]

Consistent with its pleiotropic activities, *KRIT1* is almost ubiquitously expressed in human organs and tissues, including brain, heart, liver, intestine, skeletal muscle and bone, suggesting that its deficiency may have pathophysiological consequences that extend beyond the well-known cerebrovascular effects. Accordingly, our previous studies in a mouse model demonstrated that *KRIT1* haploinsufficiency promotes oxidative and glycative stress in the liver, leading to hepatic accumulation of advanced glycation end products (AGEs) [20]. These effects correlated with a

significant downregulation of the FOXO1 transcription factor, a master regulator of energy metabolism and antioxidant responses across species [31-33]. In turn, FOXO1 downregulation was originally found to correlate with *KRIT1* knockout in mouse embryonic fibroblast (MEF) cells, along with increased levels of intracellular reactive oxygen species (ROS) and susceptibility to oxidative challenges [34], suggesting a causative relationship. Furthermore, we previously demonstrated that a high-fructose diet in *KRIT1* heterozygous (*KRIT1*$^{+/-}$) mice causes endothelial dysfunction and enhanced vascular lipid deposition, including a 2-fold increased lipid deposition in the aortic arch compared to wild-type counterpart [21].

Taken together, these results suggest that KRIT1 deficiency may have a systemic impact on intermediary metabolism–redox circuits, as well as that dietary factors may interact with KRIT1 loss to exacerbate systemic effects. Consistent with these possibilities, AGEs induced by high-fructose diets are known to activate sterol regulatory element-binding proteins (SREBPs) leading to *de novo* lipogenesis (DNL) in the liver and disrupt sphingolipid metabolism, particularly sphingosine-1-phosphate (S1P), a bioactive lipid central to pro-inflammatory and fibrotic signaling, evoking systemic oxidative stress and inflammation [35-39]. In turn, it is known that S1P signaling converges on the RhoA/ROCK mechanotransduction pathway [40-43], suggesting its potential implication in the activation of this pathway upon KRIT1 loss-of-function.

Using established *in vivo* and *in vitro* experimental models and procedures [20, 21, 44], in this study we explored whether KRIT1 haploinsufficiency affects lipid and sphingolipid metabolism and signaling in the liver, with a major focus on the S1P/RhoA/ROCK/YAP signaling cascade and associated inflammatory and fibrotic responses. Moreover, we tested the potential exacerbating effects of a high-fructose diet on such responses to unravel potential influence of challenging dietary conditions on CCM disease.

Materials and methods

Animal Model and Diet Protocol

A previously established heterozygous *KRIT1* knockout (*KRIT1*+/−) mouse model on a C57BL/6J background, generated via homologous recombination [44], was used to mimic the heterozygous condition observed in familial cerebral cavernous malformation (CCM). Male KRIT1+/− and wild-type (WT) littermates (n = 7 per group, age 26 weeks) were housed in a controlled environment (23 ± 2 °C; 13 h light/11 h dark cycle) with ad libitum access to water and standard chow.

To assess the impact of fructose on KRIT1-related metabolic alterations, mice were assigned to either a control diet (CD) or a high-fructose diet (FD, 60% fructose, Mucedola, Milan, Italy) for 22 weeks. Body weight and food/water intake were monitored weekly. At the end of the dietary intervention, mice were fasted for 4 h, anesthetized with 5% isoflurane (IsoFlo, Abbott Laboratories),

and sacrificed via cardiac puncture. Blood was collected for serum isolation, and livers were rapidly excised, snap-frozen in liquid nitrogen, and stored at –80 °C for molecular and biochemical analyses.

Lipid Profile in Plasma and Liver

Hepatic and plasma concentrations of total cholesterol and triglycerides were quantified using enzymatic colorimetric assay kits (FAR Diagnostics, Verona, Italy), according to the manufacturer's instructions.

Histological Lipid Staining (Oil Red O)

Liver cryosections (7 µm) were stained with Oil Red O to assess neutral lipid accumulation. Images were acquired using an Olympus BX41 microscope equipped with a Zeiss AxioCam MR5 digital camera at 20× magnification.

Quantification of Advanced Glycation End Products (AGEs)

The levels of Nε-carboxymethyl-lysine (CML) and pentosidine were measured in total liver protein hydrolysates using ultra-performance liquid chromatography coupled with mass spectrometry (UPLC-MS), as previously described [20]. Hydrolysis was performed with 0.6 M trichloroacetic acid and 6 M HCl for 12 h at 60 °C. Samples were analyzed using a Thermo Scientific LTQ Orbitrap mass spectrometer interfaced with a Dionex UltiMate™ 3000 HPLC system and a Phenomenex Synergi reverse-phase C18 column (150 × 2.1 mm, 3 µm). A gradient of 5 mM heptafluorobutanoic acid/acetonitrile (95/5 to 40/60 over 25 min) was used for separation. Quantification was performed using external calibration curves for CML (m/z 205.1188) and pentosidine (m/z 379.2094).

Sphingolipid Quantification

Levels of sphingosine and sphingosine-1-phosphate (S1P) were determined in liver homogenates using ultra-high-performance liquid chromatography coupled to a QTRAP 5500 triple quadrupole mass spectrometer (Sciex). Chromatographic separation was achieved using a Phenomenex Kinetex column (1.7 µm, 100 × 2.1 mm, 100 Å) and a binary gradient of solvent A (0.1% formic acid in water/acetonitrile 8:2) and solvent B (0.1% formic acid in isopropanol/acetonitrile 8:2). The elution gradient ranged from 5% to 100% B over 5 min, with a flow rate of 400 µL/min. Source conditions included an ion spray voltage of 4.5 kV and air nebulizer gas at 40/45 arbitrary units. MRM transitions were monitored as follows: sphingosine (m/z 300 → 282, CE 13%) and S1P (m/z 380 → 264, CE 21%). The lower limit of quantification was 0.50 µg/L.

Cell Culture and In Vitro Models

Mouse embryonic fibroblasts (MEFs) with homozygous deletion or lentiviral-mediated overexpression of KRIT1 were previously established (Goitre et al., 2020 PMID: 32524551). KRIT1-null MEFs (K−/−) were generated from E8.5 embryos and immortalized via the 3T3 protocol. KRIT1 was reintroduced via a pCCLsin.PPT.PGK.KRIT1.Wpre lentiviral construct, yielding a KRIT1-overexpressing line (K9/6 MEFs). MEFs were cultured in DMEM supplemented with 10% fetal calf serum, 2 mM glutamine, and 100 U/mL penicillin/streptomycin at 37 °C in a 5% CO_2 atmosphere.

Protein Extraction

For total liver proteins, tissues were homogenized (10% w/v) in RIPA buffer (50 mM Tris-HCl, pH 7.5; 150 mM NaCl; 0.5% NP-40; 0.5% sodium deoxycholate; 0.1% SDS; 10 mM EDTA; protease inhibitors). Homogenates were incubated on ice (40 min), sonicated, and centrifuged (15,000 × g, 4 °C, 40 min). Supernatants were stored at −80 °C.

For subcellular fractionation, liver homogenates were prepared in buffer containing 20 mM HEPES (pH 7.9), 1 mM $MgCl_2$, and 1% NP-40. After differential centrifugation, cytosolic and nuclear fractions were isolated as previously described [37]. Protein concentrations were measured by Bradford assay (Bio-Rad).

For cultured MEFs, protein extraction was carried out similarly using RIPA buffer with protease inhibitors, followed by centrifugation (15,000 × g, 4 °C, 20 min).

Western Blotting

Equal amounts of protein were resolved on SDS-PAGE and transferred to PVDF or nitrocellulose membranes. Membranes were blocked with 5% non-fat dry milk (NFDM) in TBS and incubated overnight at 4 °C with primary antibodies (listed in Supplementary Table 1). After washing, membranes were incubated with HRP-conjugated secondary antibodies and developed using Clarity™ Western ECL substrate (Bio-Rad). Protein bands were visualized using the ChemiDoc™ Imaging System (Bio-Rad) and quantified using Image Lab software. Signals were normalized to internal loading controls: β-actin or α-tubulin for total/cytosolic extracts, and PCNA for nuclear fractions.

Reagents

Unless otherwise specified, all reagents were of analytical grade and obtained from Sigma-Aldrich (St. Louis, MO, USA) and used without further purification.

Statistical Analysis

Data are expressed as mean ± SEM. The Shapiro–Wilk test was used to assess data normality. For comparisons between WT and KRIT1+/− groups, a two-tailed unpaired Student's t-test was applied. Statistical analysis was performed using GraphPad Prism 7.0 (GraphPad Software, San Diego, CA, USA), with $P < 0.05$ considered statistically significant.

Results

High-fructose diet potentiates AGEs accumulation and RAGE expression in KRIT1+/− mice

After 22 weeks of fructose-rich diet (FD), hepatic levels of the advanced glycation end-products (AGEs) pentosidine and Nε-carboxymethyl-lysine (CML) were significantly increased in both wild-type (WT) and KRIT1+/− (HZ) mice (Fig. 1A, B). Notably, under control diet (CD), HZ mice exhibited significantly elevated pentosidine levels compared to WT, and this increase was further exacerbated by FD (Fig. 1A). Similarly, CML levels were significantly higher in HZ-FD mice than in both WT-FD and HZ-CD groups (Fig. 1B).

Corresponding to this AGE accumulation, a marked upregulation of the receptor for AGEs (RAGE) was observed in HZ mice under CD, and further amplified following FD (Fig. 1C), suggesting a synergistic effect of KRIT1 haploinsufficiency and fructose intake on the pro-inflammatory AGE–RAGE axis.

KRIT1 haploinsufficiency and fructose intake do not alter systemic lipid profile

No significant differences in plasma triglyceride levels were observed between WT and HZ mice under either CD or FD (Fig. 2A). However, FD induced a modest but statistically significant increase in plasma cholesterol levels in WT mice, while no such effect was observed in HZ mice (Fig. 2B), indicating that systemic lipid metabolism is largely unaffected by KRIT1 haploinsufficiency.

KRIT1 loss and fructose diet synergize to activate hepatic SREBP1c and induce steatosis

Fructose and AGEs are known to activate SREBP1c, a master regulator of lipogenesis. In line with this, nuclear accumulation of active SREBP1c was significantly increased in WT-FD mice (Fig. 3A). Interestingly, HZ-CD mice already displayed elevated SREBP1c activation compared to WT-CD, and this effect was further amplified by FD.

These changes correlated with increased hepatic triglyceride content in WT-FD, HZ-CD, and HZ-FD groups compared to WT-CD (Fig. 3B). Histological analysis by Oil Red O staining confirmed the biochemical findings, revealing focal periportal macrovesicular steatosis in WT-FD mice, and more

extensive microvesicular steatosis in HZ mice under both diets, particularly exacerbated by FD (Fig. 3C).

KRIT1 loss and fructose synergistically activate SREBP2/mevalonate pathway and downstream RhoA/ROCK/YAP signaling

SREBP2, which regulates cholesterol biosynthesis, was significantly activated (nuclear translocation) in both WT-FD and HZ-CD mice compared to WT-CD, with a further increase in HZ-FD mice (Fig. 4A). Consistently, hepatic levels of HMG-CoA reductase (HMG-CoA-R), a key SREBP2 target, were significantly higher in HZ-FD mice than WT-FD (Fig. 4B).

Activation of the SREBP2 pathway was associated with a decrease in phosphorylated (inactive) RhoA (Fig. 4C), increased ROCK1 expression (Fig. 4D), and reduced phosphorylation of YAP (Fig. 4E), promoting its nuclear translocation and transcriptional activity. Although not statistically significant, FD appeared to further enhance this activation cascade in HZ mice.

KRIT1 loss alters sphingosine-1-phosphate metabolism in a diet-dependent manner

Given the link between YAP activation and sphingosine-1-phosphate (S1P) signaling, we next assessed hepatic S1P metabolism. Total sphingosine levels remained unchanged across all groups (Fig. 5A). However, S1P levels were significantly elevated in HZ-CD mice versus WT-CD, and FD also increased S1P in WT mice (Fig. 5B). Strikingly, S1P levels in HZ-FD mice did not differ from those in HZ-CD or WT-CD mice.

Protein levels of sphingosine kinase 1 (SphK1) were elevated in WT-FD and HZ-CD groups relative to WT-CD, but dramatically reduced in HZ-FD mice (Fig. 5C). Conversely, SphK2 levels were unaffected by FD in WT mice but significantly increased in HZ mice under both diets (Fig. 5D).

S1PR1 expression mirrored SphK1 trends: increased in WT-FD and HZ-CD mice, but suppressed in HZ-FD (Fig. 5E). In contrast, S1PR3 levels were significantly upregulated in HZ-CD mice and further increased by FD, with no significant effect observed in WT groups (Fig. 5F). These data suggest a complex interplay between KRIT1 loss and fructose intake in modulating S1P signaling components.

KRIT1 loss and fructose intake promote hepatic inflammation and fibrosis

To assess downstream consequences of RAGE and YAP activation, we evaluated key markers of inflammation and fibrosis. TLR4 expression, a sensor of both AGEs and mechanical stress, was significantly upregulated by both KRIT1 loss and FD, with an additive effect in HZ-FD mice (Fig. 6A). Similarly, IL-1β levels were elevated in HZ-CD and WT-FD mice, and highest in HZ-FD (Fig. 6B).

TGF-β expression showed a non-significant trend toward increase in WT-FD and HZ-CD mice versus WT-CD (Fig. 6C), while fibronectin levels, a late marker of fibrosis, were modestly elevated in WT-FD and HZ-CD groups, but markedly increased in HZ-FD mice (Fig. 6D), supporting a synergistic pro-fibrotic effect of KRIT1 loss and fructose feeding.

KRIT1 gene modulation regulates lipid and inflammatory pathways in MEF cells

To confirm the direct role of KRIT1 in lipid and inflammatory signaling, we analyzed MEF cells with complete KRIT1 knockout (K−/−) and KRIT1 re-expression (K9/6). Compared to K9/6, K−/− cells displayed elevated levels of active SREBP1c and SREBP2, as well as HMG-CoA-R (Fig. 7A). SphK1 was upregulated, while SphK2 was downregulated in K−/− cells relative to KRIT1-overexpressing controls (Fig. 7B).

Consistently, S1PR1 expression was reduced and S1PR3 increased in K−/− cells (Fig. 7C). TLR4 and fibronectin were also elevated, whereas TGF-β was suppressed in the absence of KRIT1, with all trends reversed upon KRIT1 re-expression (Fig. 7D), confirming the regulatory role of KRIT1 in metabolic and inflammatory responses.

Discussion

In this study, we identify a previously unrecognized role of KRIT1 in the regulation of hepatic lipid and sphingolipid metabolism, providing evidence that KRIT1 haploinsufficiency is sufficient to prime the liver toward a steatotic, pro-inflammatory and pro-fibrotic phenotype that is markedly exacerbated by a high-fructose diet.

The main finding emerging from our data is that KRIT1 loss does not simply reproduce a vascular defect outside the brain, but rather establishes a broader metabolic vulnerability characterized by AGE accumulation, activation of SREBP-dependent lipid and mevalonate pathways, remodelling of S1P signalling, and engagement of the RhoA/ROCK/YAP axis. These results therefore extend the pathological framework of KRIT1-associated disease beyond the cerebrovascular compartment and support the concept that environmental metabolic stressors may interact with genetically determined redox and metabolic fragility. This interpretation is consistent with our previous study showing that KRIT1 haploinsufficiency affects hepatic metabolic functions, reduces FoxO1-dependent signalling, promotes hepatic AGE accumulation, and alters antioxidant/antiglycative defences *in vivo* and in KRIT1 knockout cells [20].

A relevant aspect of the present study is the absence of major systemic lipid alterations in our model whereas liver tissue displayed clear biochemical and histological evidence of lipid accumulation strengthening the conclusion that KRIT1 deficiency induces a tissue-specific metabolic imbalance evoking hepasteatosis, already evident under basal conditions.

The upstream driver of this phenotype may be represented by a redox-glycative imbalance. Previous work from our group demonstrated that KRIT1 haploinsufficiency promotes hepatic oxidative and glycative stress, leading to AGE accumulation and FOXO1 downregulation, while in another study from our group KRIT1 deletion in mice aggravates vascular lipid deposition induced by fructose feeding [20, 21]. In the present study, fructose and KRIT1 loss converge on activation of the hepatic AGE/RAGE axis. Pentosidine levels were already elevated in HZ mice under control diet, whereas CML and RAGE expression were particularly enhanced in HZ-FD animals, indicating that KRIT1 deficiency lowers the threshold for fructose-induced glycoxidative stress. This interpretation is supported by experimental evidence showing that fructose-derived AGEs can promote lipogenic reprogramming through dysregulation of SREBP-1c and that inhibition of AGE generation counteracts fructose-induced metabolic alterations [36]. Moreover, in fructose-drinking mice, hepatic CML accumulation was associated with activation of the SCAP/SREBP pathway and hepatosteatosis, supporting a direct mechanistic connection between fructose-derived glycation products and lipogenic signalling [45]. Within this framework, fructose may function not merely as a substrate for lipogenesis but as a metabolic amplifier of a pre-existing KRIT1-dependent vulnerability to glycative stress.

Indeed, downstream of AGE/RAGE activation, our data indicate a coordinated induction of SREBP1c-mediated lipogenesis and SREBP2-dependent mevalonate signalling. KRIT1-deficient mice showed increased nuclear SREBP1c accumulation and hepatic triglyceride deposition, effects that were further enhanced by fructose feeding. In parallel, activation of SREBP2 and increased HMG-CoA reductase expression pointed to stimulation of the mevalonate pathway. This observation is particularly relevant because mevalonate-derived isoprenoid intermediates are required for prenylation and activation of small GTPases, including RhoA. Thus, enhanced SREBP2/mevalonate signalling may provide an additional mechanism linking metabolic dysregulation to sustained RhoA/ROCK activation. Although most studies on RhoA/ROCK in CCM have focused on endothelial cells, original and translational work has shown that ROCK inhibition reduces lesion burden in murine CCM models, supporting the centrality of this pathway in CCM pathogenesis [10, 16, 26]. More recently, patient-derived induced pluripotent stem cells (iPSCs) models carrying heterozygous KRIT1 mutations showed endothelial junctional defects and abnormal transcriptional phenotypes, further supporting the biological impact of KRIT1 haploinsufficiency itself [46]. Our findings therefore suggest that activation of the mevalonate pathway may reinforce KRIT1-dependent pathogenic signalling through a metabolic route that operates beyond the cerebral vasculature.

The observation that KRIT1 haploinsufficiency activates the RhoA/ROCK/YAP pathway in the liver provides a direct mechanistic connection between metabolic dysfunction and both CCM biology and hepatic fibrogenesis. Reduced phosphorylation of inactive RhoA, increased ROCK1 expression and enhanced YAP activation occurred in parallel with mevalonate pathway induction, suggesting functional integration of these signalling modules. In liver disease, YAP/TAZ signalling has emerged

as a key regulator of tissue remodelling and fibrogenesis. Experimental studies demonstrated that YAP activation drives hepatic stellate cell activation and fibrosis [47], whereas hepatocyte-specific TAZ/YAP signalling promotes the transition from steatosis to steatohepatitis and fibrotic liver injury [48, 49]. More recently, hepatocyte-targeted silencing of TAZ was shown to attenuate liver inflammation and fibrosis in humanized NASH models, further supporting the pathogenic role of Hippo pathway dysregulation in progressive metabolic liver disease [50]. Thus, the experimental evidence linking YAP to fibrotic remodelling supports the interpretation that aberrant activation of this pathway may contribute to extracellular matrix deposition in KRIT1-deficient liver. In this context, the same signalling machinery classically implicated in CCM vascular instability may be redeployed in hepatic cells to promote inflammation, matrix remodelling and tissue injury.

A further major finding of the present study is that KRIT1 profoundly modulates hepatic sphingolipid signalling. S1P levels were significantly increased in HZ-CD mice and in WT-FD animals, indicating that either KRIT1 loss or fructose exposure is sufficient to enhance S1P production. Interestingly, the combined condition did not result in a further increase in total S1P but instead was characterized by a marked reduction in SphK1 and S1PR1 together with sustained or enhanced SphK2 and S1PR3 expression. These findings suggest that KRIT1 loss does not simply increase sphingolipid flux, but alters the balance among distinct branches of the S1P signalling network. This is particularly relevant because a recent original study demonstrated that S1P levels are increased in MASH livers, that SphK1 expression rises in human MASH samples, and that S1P stimulates hepatic stellate cell activation, thereby promoting fibrotic remodelling [51].

The apparent induction of the SphK1/S1PR1 axis observed in WT-FD and HZ-CD mice may represent an adaptive response to metabolic stress. By contrast, the suppression of this response in HZ-FD mice, together with further induction of SphK2 and S1PR3, points to a maladaptive switch toward a more inflammatory and fibrogenic signalling profile. In this regard, the specific increase in S1PR3 is particularly intriguing. While S1PR1 predominantly mediates barrier-protective and homeostatic responses through Gi/Rac1 signalling, S1PR3 preferentially engages RhoA-dependent pathways that promote vascular permeability, inflammatory activation and tissue remodelling, particularly under conditions of chronic sphingolipid stress [52, 53]. Our findings therefore support a model in which KRIT1 haploinsufficiency promotes a shift from a potentially compensatory S1PR1-dominated response toward S1PR3-driven signalling, thereby reinforcing RhoA/ROCK/YAP activation and tissue remodelling. Although direct evidence on S1PR3 in KRIT1-deficient liver is not currently available, original studies in NASH models demonstrate that S1P receptor modulation can alter hepatic inflammation and immune-cell recruitment, supporting the broader relevance of S1P receptor signalling in metabolic liver disease [54]. Indeed, a growing evidence implicating sphingolipid metabolism in steatohepatitis progression and fibrosis. In a recent spatial multi-omics study, sphingolipid metabolism was shown to be dysregulated in fibrotic liver regions, sphingolipid-related genes were enriched in non-parenchymal cells, and pharmacological inhibition of

sphingolipid pathways exerted anti-fibrotic effects in hepatic stellate cells and human precision-cut liver slices [55]. In another original study, hepatic sphingomyelin phosphodiesterase 3 (SMPD3) was identified as a driver of MASH progression through sphingomyelin hydrolysis, ceramide accumulation, caveolae-dependent lipid uptake, extracellular vesicle release, inflammation and fibrosis [56]. Together with our data, these observations place KRIT1 within a broader metabolic network in which sphingolipid remodelling serves as a critical bridge between lipid stress, inflammatory signalling and fibrosis.

The S1P receptor switch observed in our model may also help explain the inflammatory and fibrotic phenotype observed downstream. TLR4 expression was increased by both KRIT1 loss and fructose, with further enhancement in HZ-FD mice, while IL-1β and fibronectin followed a similar pattern. These findings indicate that the metabolic alterations induced by KRIT1 haploinsufficiency translate into biologically relevant inflammatory and profibrotic responses. In this context, fibronectin accumulation in HZ-FD mice may represent the final outcome of a signalling cascade involving AGE/RAGE activation, SREBP-driven metabolic reprogramming, S1P receptor remodelling and YAP-mediated transcriptional responses. This interpretation is also consistent with our recent demonstration that pharmacological inhibition of AGE formation attenuates diet-induced metaflammation through modulation of S1P/RhoA/ROCK signalling, supporting the notion that glycative stress and sphingolipid pathways are mechanistically interconnected [37, 57].

An important strength of the study is the validation of KRIT1-dependent regulation in cellular models. KRIT1-null MEFs displayed increased SREBP1c, SREBP2 and HMG-CoA reductase expression, altered S1P signalling components, and enhanced inflammatory and fibrotic markers compared with KRIT1-reexpressing cells. Reversal of these alterations by KRIT1 re-expression supports a direct role of KRIT1 in controlling lipid, sphingolipid and inflammatory pathways rather than reflecting purely secondary effects of diet or tissue context. Although MEFs cannot fully recapitulate liver physiology, these findings provide mechanistic support for the concept that KRIT1 functions as a broader metabolic-redox regulator in multiple cell types.

Taken together, these results support a working model in which KRIT1 haploinsufficiency establishes a primed hepatic state characterized by impaired redox and glycative control, enhanced lipogenic activity and S1P pathway remodelling. When fructose intake is superimposed, glycoxidative stress further amplifies these pathways, promotes activation of RhoA/ROCK/YAP signalling and shifts the S1P network toward a SphK2/S1PR3-dominant profile associated with inflammation and fibrosis. In this model, KRIT1 acts not only as a regulator of endothelial stability but also as a systemic modulator of metabolic resilience.

The broader implication of this model is that CCM disease expression may be influenced by systemic metabolic status. Our findings suggest that high intake of reducing sugars may represent a disease-modifying stressor in individuals carrying KRIT1 mutations, not because hepatic alterations directly cause cerebral lesions, but because KRIT1 deficiency generates a systemic pro-oxidant, pro-

glycative and pro-inflammatory environment that may affect multiple tissues. From a translational perspective, future studies should assess whether KRIT1 mutation carriers display altered hepatic metabolic profiles or increased susceptibility to MASLD/MASH and whether interventions targeting AGE/RAGE signalling, the mevalonate pathway or S1P-mediated signalling may provide therapeutic benefit. Further mechanistic studies will also be required to define the causal hierarchy among the signalling pathways identified here and to determine their relevance in human disease.

Conclusions

Collectively, this study reveals KRIT1 as a previously unrecognized regulator of hepatic lipid and sphingolipid homeostasis. Our findings demonstrate for the first time that KRIT1 haploinsufficiency promotes hepatic AGE/RAGE activation, SREBP1c-driven lipogenesis, mevalonate pathway induction, S1P receptor remodelling and RhoA/ROCK/YAP signalling driving hepatic inflammation and fibrosis. In this context, a fructose-rich diet acts as a second metabolic hit that amplifies these alterations, raising the possibility that individuals carrying KRIT1 mutations have increased susceptibility to fatty liver, steatohepatitis, and CCM lesion progression, especially under high-sugar dietary conditions. These findings, thus, broaden the biological significance of KRIT1 beyond the cerebral endothelium highlighting the systemic nature of KRIT1-mediated disease and support a model in which genetic susceptibility and metabolic stress cooperate to shape disease expression.

In this perspective, clinical strategies targeting metabolic pathways (e.g., limiting dietary AGEs, statin therapy, S1P/S1PR3 modulation) could offer dual benefits for hepatic health and CCM management. Future epidemiological and interventional studies are needed to assess metabolic comorbidities and to validate dietary or pharmacological guidelines for individuals with KRIT1 mutations.

Funding: This research was funded by the Telethon Foundation (grant GGP15219 to SFR), the Fondazione CRT (Cassa di Risparmio di Torino) (project grant “Cerebro-NGS.TO” to SFR), the Università degli Studi di Torino (Local Research Funding 2018-21 to RM and SFR).

Competing Interests: The authors have no financial or non-financial interests to disclose.

Author Contributions: Conceptualization: RM, and SFR. Methodology: RM, FDB, LG and SFR. Investigation: GC, AP, CF, FDB, ASC. Data curation and figure preparation: RM, GC and AP. Writing-original draft preparation: RM and SFR. Writing-review and editing: RM and SFR. Supervision and project administration: SFR. Funding acquisition: SFR and RM. All authors have read and agreed to the submitted version of the manuscript.

Data Availability Statement: Data are available on motivated request from the corresponding authors.

Ethics approval: The animal care and experimental use protocol followed the guidelines of the European Directive 2010/63/EU on the protection of animals used for scientific purposes, and was approved by the local Animal Use and Care Committee of the University of Torino (Torino, Italy) and the Italian Ministry of Health (authorization number: 350/2019-PR).

Acknowledgments: The authors are grateful to CCM Italia, the Italian Research Network for Cerebral Cavernous Malformation (https://www.ccmitalia.unito.it), and the Associazione Italiana Angiomi Cavernosi (AIAC) Onlus (https: //www.aiac.unito.it), including its president Massimo Chiesa, for fundamental support.

Use of artificial intelligence-assisted technologies: Microsoft Copilot was used solely to support language editing and improve the clarity and organization of the manuscript text. No AI tools were used for study design, data analysis, data interpretation, figure preparation, or generation of scientific conclusions.

Abbreviations: AGEs, advanced glycation end-products; CCM, Cerebral Cavernous Malformation; CML, Nε-carboxymethyl-lysine; HMG-CoA-R, hydroxy-methyl-glutaryl coenzyme A reductase; IL-1β, interleukin-1β; KRIT1, Krev interaction trapped 1; MEFs, mouse embryonic fibroblasts; RAGE, receptors of AGE; RhoA, Ras homolog family member A; ROCK, Rho associated coiled-coil containing protein kinase 1; S1P, sphingosine-1-phosphate; S1PRs, sphingosine-1-phosphate receptors; Sph, sphingosine; SphKs, sphingosine kinases; SREBPs, sterol regulatory element binding proteins; TGF-β, transforming growth factor β; TLR4, Toll-like receptor 4; TNF-α, tumor necrosis factor alpha; YAP, yes-associated protein 1; WT, wild-type.

References

1. Retta SF, Balzac F, Avolio M (2006) Rap1: a turnabout for the crosstalk between cadherins and integrins. Eur J Cell Biol 85(3-4):283-93.
2. Serebriiskii I, Estojak J, Sonoda G, Testa JR, Golemis EA (1997) Association of Krev-1/rap1a with Krit1, a novel ankyrin repeat-containing protein encoded by a gene mapping to 7q21-22. Oncogene 15(9):1043-9.

3. Laberge-le Couteulx S, Jung HH, Labauge P et al (1999) Truncating mutations in CCM1, encoding KRIT1, cause hereditary cavernous angiomas. Nat Genet 23(2):189-93.
4. Sahoo T, Johnson EW, Thomas JW et al (1999) Mutations in the gene encoding KRIT1, a Krev-1/rap1a binding protein, cause cerebral cavernous malformations (CCM1). Hum Mol Genet 8(12):2325-33.
5. Batra S, Lin D, Recinos PF, Zhang J, Rigamonti D (2009) Cavernous malformations: natural history, diagnosis and treatment. Nat Rev Neurol 5(12):659-70.
6. Flemming KD (2020) Incidence, Prevalence, and Clinical Presentation of Cerebral Cavernous Malformations. Methods Mol Biol 2152:27-33.
7. Tournier-Lasserve E (2020) Molecular Genetic Screening of CCM Patients: An Overview. Methods Mol Biol 2152:49-57.
8. Borikova AL, Dibble CF, Sciaky N et al (2010) Rho kinase inhibition rescues the endothelial cell cerebral cavernous malformation phenotype. J Biol Chem 285(16):11760-4.
9. Glading A, Han J, Stockton RA, Ginsberg MH (2007) KRIT-1/CCM1 is a Rap1 effector that regulates endothelial cell cell junctions. J Cell Biol 179(2):247-54.
10. Stockton RA, Shenkar R, Awad IA, Ginsberg MH (2010) Cerebral cavernous malformations proteins inhibit Rho kinase to stabilize vascular integrity. J Exp Med 207(4):881-96.
11. Perrelli A, Ferraris C, Berni E, Glading AJ, Retta SF (2023) KRIT1: A Traffic Warden at the Busy Crossroads Between Redox Signaling and the Pathogenesis of Cerebral Cavernous Malformation Disease. Antioxid Redox Signal 38(7-9):496-528.
12. Richardson BT, Dibble CF, Borikova AL, Johnson GL (2013) Cerebral cavernous malformation is a vascular disease associated with activated RhoA signaling. Biol Chem 394(1):35-42.
13. Whitehead KJ, Chan AC, Navankasattusas S et al (2009) The cerebral cavernous malformation signaling pathway promotes vascular integrity via Rho GTPases. Nat Med 15(2):177-84.
14. Ayata C, Kim H, Morrison L et al (2024) Role of Rho-Associated Kinase in the Pathophysiology of Cerebral Cavernous Malformations. Neurol Genet 10(1):e200121.
15. Li DY, Whitehead KJ (2010) Evaluating strategies for the treatment of cerebral cavernous malformations. Stroke 41(10 Suppl):S92-4.
16. McDonald DA, Shi C, Shenkar R et al (2012) Fasudil decreases lesion burden in a murine model of cerebral cavernous malformation disease. Stroke 43(2):571-4.
17. Shenkar R, Shi C, Austin C et al (2017) RhoA Kinase Inhibition With Fasudil Versus Simvastatin in Murine Models of Cerebral Cavernous Malformations. Stroke 48(1):187-94.
18. Antognelli C, Trapani E, Delle Monache S et al (2018) KRIT1 loss-of-function induces a chronic Nrf2-mediated adaptive homeostasis that sensitizes cells to oxidative stress: Implication for Cerebral Cavernous Malformation disease. Free Radic Biol Med 115:202-18.
19. Bianconi A, Salvati LF, Perrelli A et al (2022) Distant Recurrence of a Cerebral Cavernous Malformation in the Vicinity of a Developmental Venous Anomaly: Case Report of Local Oxy-Inflammatory Events. Int J Mol Sci 23(23).
20. Mastrocola R, Aimaretti E, Ferreira Alves G et al (2022) Heterozygous Loss of KRIT1 in Mice Affects Metabolic Functions of the Liver, Promoting Hepatic Oxidative and Glycative Stress. Int J Mol Sci 23(19).
21. Vieceli Dalla Sega F, Mastrocola R, Aquila G et al (2019) KRIT1 Deficiency Promotes Aortic Endothelial Dysfunction. Int J Mol Sci 20(19).
22. Choquet H, Trapani E, Goitre L et al (2016) Cytochrome P450 and matrix metalloproteinase genetic modifiers of disease severity in Cerebral Cavernous Malformation type 1. Free Radic Biol Med 92:100-9.

23. Perrelli A, Retta SF (2021) Polymorphisms in genes related to oxidative stress and inflammation: Emerging links with the pathogenesis and severity of Cerebral Cavernous Malformation disease. Free Radic Biol Med 172:403-17.

24. Trapani E, Retta SF (2015) Cerebral cavernous malformation (CCM) disease: from monogenic forms to genetic susceptibility factors. J Neurosurg Sci 59(3):201-9.

25. De Luca E, Pedone D, Moglianetti M et al (2018) Multifunctional Platinum@BSA-Rapamycin Nanocarriers for the Combinatorial Therapy of Cerebral Cavernous Malformation. ACS Omega 3(11):15389-98.

26. Gibson CC, Zhu W, Davis CT et al (2015) Strategy for identifying repurposed drugs for the treatment of cerebral cavernous malformation. Circulation 131(3):289-99.

27. Kim HA, Perrelli A, Ragni A et al (2020) Vitamin D Deficiency and the Risk of Cerebrovascular Disease. Antioxidants (Basel) 9(4).

28. Marchi S, Trapani E, Corricelli M et al (2016) Beyond multiple mechanisms and a unique drug: Defective autophagy as pivotal player in cerebral cavernous malformation pathogenesis and implications for targeted therapies. Rare Dis 4(1):e1142640.

29. Retta SF, Glading AJ (2016) Oxidative stress and inflammation in cerebral cavernous malformation disease pathogenesis: Two sides of the same coin. Int J Biochem Cell Biol 81(Pt B):254-70.

30. Retta SF, Perrelli A, Trabalzini L, Finetti F (2020) From Genes and Mechanisms to Molecular-Targeted Therapies: The Long Climb to the Cure of Cerebral Cavernous Malformation (CCM) Disease. Methods Mol Biol 2152:3-25.

31. de Keizer PL, Burgering BM, Dansen TB (2011) Forkhead box o as a sensor, mediator, and regulator of redox signaling. Antioxid Redox Signal 14(6):1093-106.

32. Kousteni S (2012) FoxO1, the transcriptional chief of staff of energy metabolism. Bone 50(2):437-43.

33. Krafczyk N, Klotz LO (2022) FOXO transcription factors in antioxidant defense. IUBMB Life 74(1):53-61.

34. Goitre L, Balzac F, Degani S et al (2010) KRIT1 regulates the homeostasis of intracellular reactive oxygen species. PLoS One 5(7):e11786.

35. Bhattacharjee P, Fadlaoui A, Ryan CE et al (2025) Induction of Fructose Mediated De Novo Lipogenesis Coexists with the Upregulation of Mitochondrial Oxidative Function in Mice Livers. J Nutr 155(6):1768-81.

36. Mastrocola R, Collino M, Nigro D et al (2015) Accumulation of advanced glycation end-products and activation of the SCAP/SREBP Lipogenetic pathway occur in diet-induced obese mouse skeletal muscle. PLoS One 10(3):e0119587.

37. Mastrocola R, Dal Bello F, Cento AS et al (2021) Altered hepatic sphingolipid metabolism in insulin resistant mice: Role of advanced glycation endproducts. Free Radic Biol Med 169:425-35.

38. Nigro D, Menotti F, Cento AS et al (2017) Chronic administration of saturated fats and fructose differently affect SREBP activity resulting in different modulation of Nrf2 and Nlrp3 inflammasome pathways in mice liver. J Nutr Biochem 42:160-71.

39. Todoric J, Di Caro G, Reibe S et al (2020) Fructose stimulated de novo lipogenesis is promoted by inflammation. Nat Metab 2(10):1034-45.

40. Brand CS, Tan VP, Brown JH, Miyamoto S (2018) RhoA regulates Drp1 mediated mitochondrial fission through ROCK to protect cardiomyocytes. Cell Signal 50:48-57.

41. Medlin MD, Staus DP, Dubash AD, Taylor JM, Mack CP (2010) Sphingosine 1-phosphate receptor 2 signals through leukemia-associated RhoGEF (LARG), to promote smooth muscle cell differentiation. Arterioscler Thromb Vasc Biol 30(9):1779-86.

42. Park S, Kim J, Yang S et al (2024) Exogenous S1P via S1P receptor 2 induces CTGF expression through Src-RhoA-ROCK-YAP pathway in hepatic stellate cells. Mol Biol Rep 51(1):950.
43. Yung BS, Brand CS, Xiang SY et al (2017) Selective coupling of the S1P(3) receptor subtype to S1P-mediated RhoA activation and cardioprotection. J Mol Cell Cardiol 103:1-10.
44. Goitre L, Fornelli C, Zotta A, Perrelli A, Retta SF (2020) Production of KRIT1-knockout and KRIT1-knockin Mouse Embryonic Fibroblasts as Cellular Models of CCM Disease. Methods Mol Biol 2152:151-67.
45. Mastrocola R, Collino M, Rogazzo M et al (2013) Advanced glycation end products promote hepatosteatosis by interfering with SCAP-SREBP pathway in fructose-drinking mice. Am J Physiol Gastrointest Liver Physiol 305(6):G398-407.
46. Arce M, Erzar I, Yang F et al (2025) KRIT1 heterozygous mutations are sufficient to induce a pathological phenotype in patient-derived iPSC models of cerebral cavernous malformation. Cell Rep 44(5):115576.
47. Mannaerts I, Leite SB, Verhulst S et al (2015) The Hippo pathway effector YAP controls mouse hepatic stellate cell activation. J Hepatol 63(3):679-88.
48. Salloum S, Jeyarajan AJ, Kruger AJ et al (2021) Fatty Acids Activate the Transcriptional Coactivator YAP1 to Promote Liver Fibrosis via p38 Mitogen-Activated Protein Kinase. Cell Mol Gastroenterol Hepatol 12(4):1297-310.
49. Wang X, Zheng Z, Caviglia JM et al (2016) Hepatocyte TAZ/WWTR1 Promotes Inflammation and Fibrosis in Nonalcoholic Steatohepatitis. Cell Metab 24(6):848-62.
50. Wang X, Moore MP, Shi H et al (2023) Hepatocyte-targeted siTAZ therapy lowers liver fibrosis in NASH diet-fed chimeric mice with hepatocyte-humanized livers. Mol Ther Methods Clin Dev 31:101165.
51. Osawa Y, Kawai H, Nakashima K et al (2024) Sphingosine-1-phosphate promotes liver fibrosis in metabolic dysfunction-associated steatohepatitis. PLoS One 19(5):e0303296.
52. Singleton PA, Dudek SM, Ma SF, Garcia JG (2006) Transactivation of sphingosine 1-phosphate receptors is essential for vascular barrier regulation. Novel role for hyaluronan and CD44 receptor family. J Biol Chem 281(45):34381-93.
53. Sugimoto N, Takuwa N, Okamoto H, Sakurada S, Takuwa Y (2003) Inhibitory and stimulatory regulation of Rac and cell motility by the G12/13-Rho and Gi pathways integrated downstream of a single G protein-coupled sphingosine-1-phosphate receptor isoform. Mol Cell Biol 23(5):1534-45.
54. Liao CY, Barrow F, Venkatesan N et al (2023) Modulating sphingosine 1-phosphate receptor signaling skews intrahepatic leukocytes and attenuates murine nonalcoholic steatohepatitis. Front Immunol 14:1130184.
55. Gruevska A, Leslie J, Perpiñán E et al (2025) Spatial lipidomics reveals sphingolipid metabolism as anti-fibrotic target in the liver. Metabolism 168:156237.
56. Jiang J, Gao Y, Wang J et al (2025) Hepatic sphingomyelin phosphodiesterase 3 promotes steatohepatitis by disrupting membrane sphingolipid metabolism. Cell Metab 37(5):1119-36.e13.
57. Rivas Navarrete PI, Collotta D, Dal Bello F et al (2025) Inhibition of advanced glycation end-products by the vitamin B6 vitamer pyridoxamine prevents systemic and skeletal muscle diet-induced metaflammation through modulation of S1P/RhoA/ROCK signalling. J Nutr Biochem 146:110068.

Figure legends

Figure 1. High-fructose diet exacerbates AGEs accumulation and RAGE upregulation in KRIT1+/– mice. Quantification of hepatic pentosidine (A) and Nε-carboxymethyl-lysine (CML) (B) by UPLC-MS in wild-type (WT) and KRIT1 heterozygous (HZ) mice after 22 weeks of control diet (CD) or high-fructose diet (FD). (C) Representative Western blot of RAGE protein expression in liver homogenates. Densitometric analyses represent band intensities normalized to α-tubulin and expressed as fold-change relative to WT-CD. Data are presented as mean ± SEM (n = 7 per group). *P<0.05; **P<0.005; ***P<0.001.

Figure 2. Plasma lipid profile remains unchanged by KRIT1 haploinsufficiency and fructose feeding. Plasma triglyceride (A) and cholesterol (B) levels in WT and HZ mice after 22 weeks of CD or FD. While triglycerides remained unchanged, FD induced a mild but significant increase in cholesterol in WT mice. Data are presented as mean ± SEM (n = 7 per group). *P<0.05.

Figure 3. SREBP1c activation and hepatic lipid accumulation are enhanced by KRIT1 loss and high-fructose diet. (A) Representative Western blot of nuclear active SREBP1c in liver nuclear extracts of WT and HZ mice under CD or FD. Densitometric values are normalized to PCNA and expressed as fold-change relative to WT-CD. (B) Hepatic triglyceride content determined by biochemical analysis. (C) Representative Oil Red O staining of liver sections showing neutral lipid accumulation; WT-FD livers exhibit focal macrovesicular steatosis, while HZ livers show diffuse microvesicular steatosis, further intensified by FD. Data are presented as mean ± SEM (n = 7 per group). *P<0.05; **P<0.005.

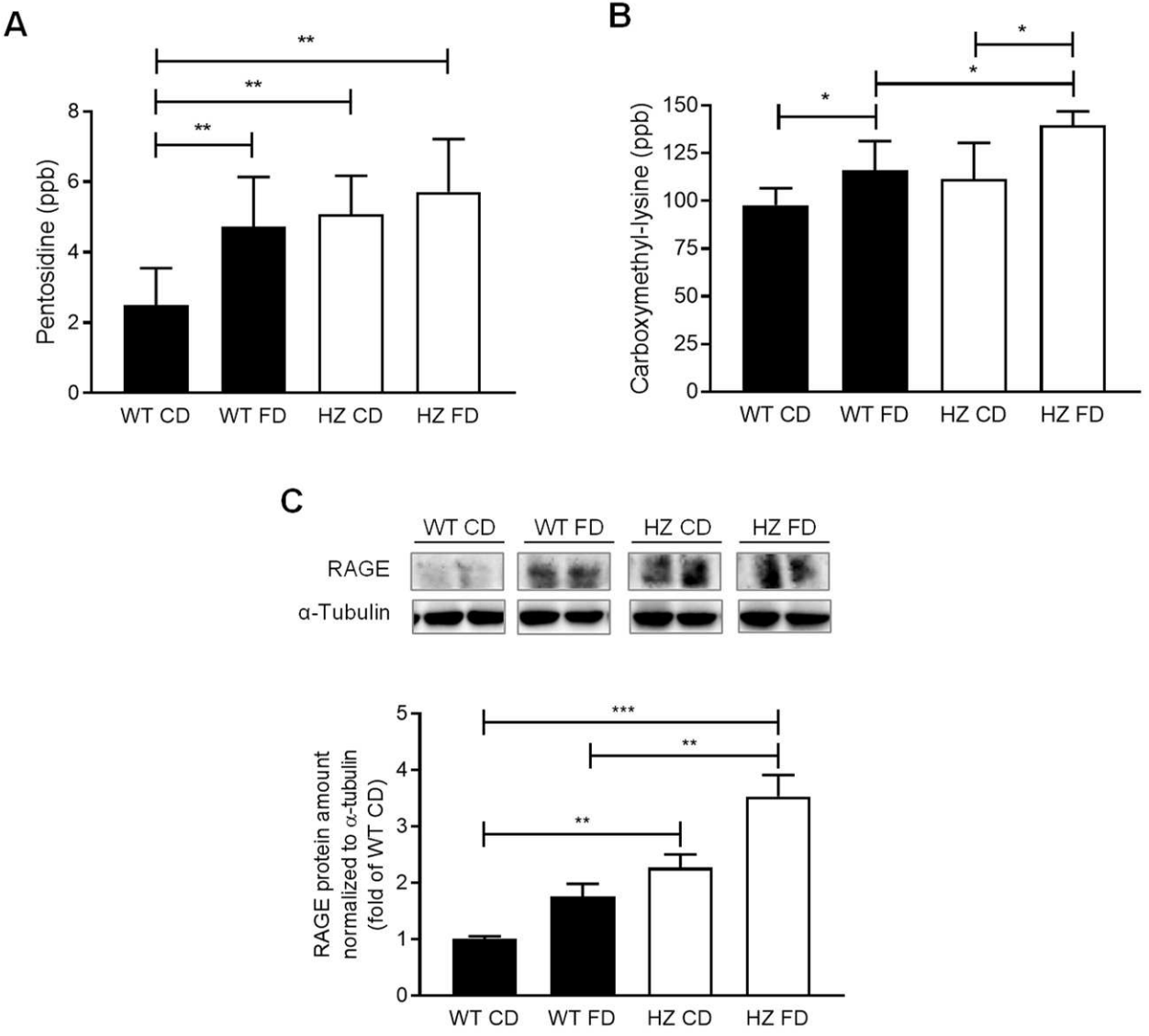
Figure 4. Synergistic activation of SREBP2/mevalonate and RhoA/ROCK/YAP pathways in KRIT1+/– mice fed fructose. Representative Western blots showing: (A) nuclear active SREBP2, (B) HMG-CoA reductase (HMG-CoA-R), (C) RhoA phosphorylated at Ser188 and total RhoA, (D) ROCK1, and (E) phosphorylated YAP in liver extracts from WT and HZ mice under CD or FD. Densitometric analyses are normalized to PCNA (for nuclear proteins) or α-tubulin (for cytosolic proteins), and reported as fold-change relative to WT-CD. Data are presented as mean ± SEM (n = 7 per group). *P<0.05; **P<0.005.

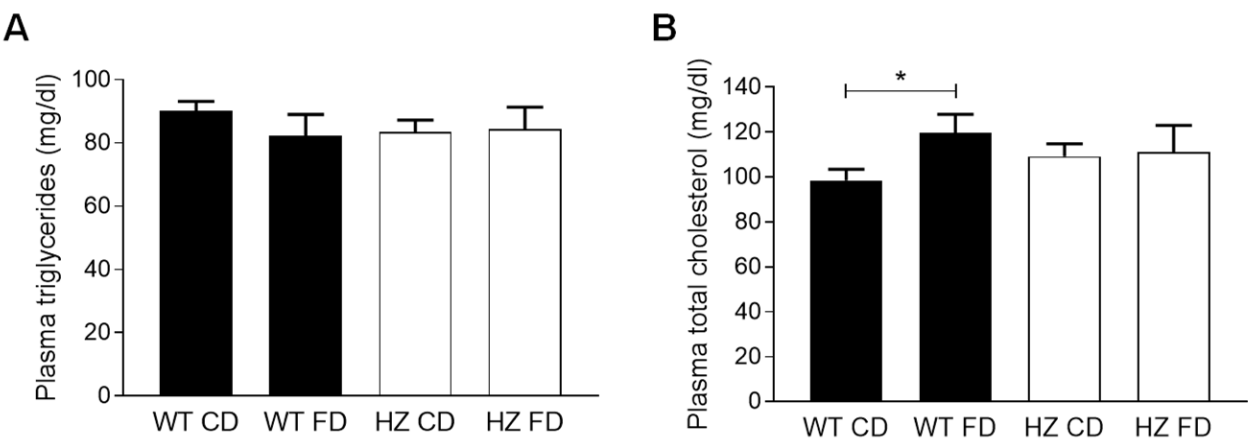
Figure 5. KRIT1 loss and fructose intake differentially modulate hepatic S1P metabolism and signaling. UPLC-MS quantification of (A) sphingosine (Sph) and (B) sphingosine-1-phosphate (S1P) in liver homogenates of WT and HZ mice under CD or FD. (C–F) Representative Western blots of SphK1 and SphK2

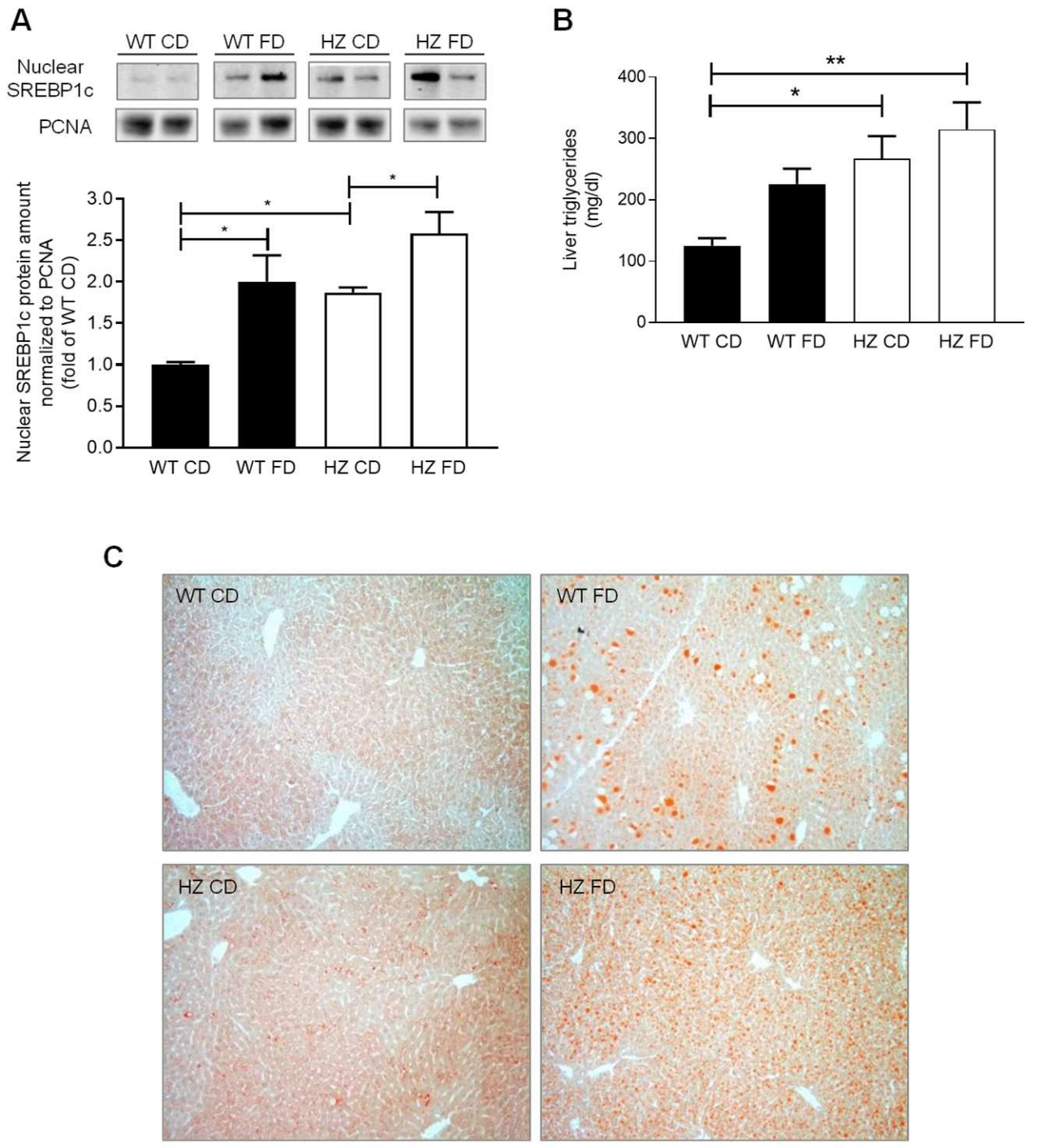
(S1P-producing enzymes), and S1PR1 and S1PR3 (S1P receptors) in liver tissue. Densitometric values are normalized to α-tubulin and expressed as fold-change relative to WT-CD. Data are presented as mean ± SEM (n = 7 per group). *P<0.05; **P<0.005; ***P<0.001.

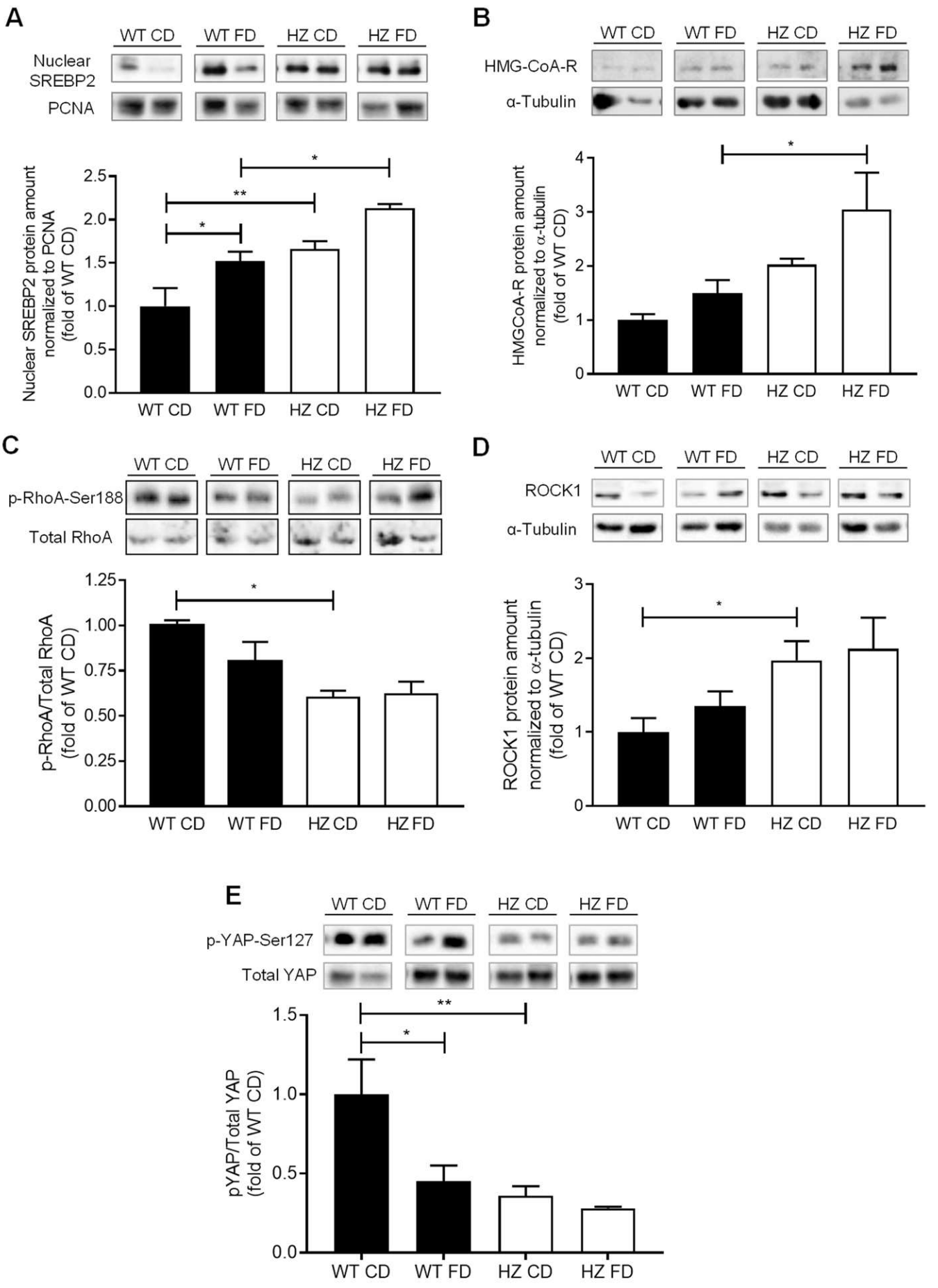
Figure 6. KRIT1 haploinsufficiency and fructose feeding promote hepatic inflammation and fibrosis. Representative Western blots showing hepatic expression of: (A) TLR4, (B) IL-1β, (C) TGF-β, and (D) fibronectin in WT and HZ mice after 22 weeks of CD or FD. Densitometric analyses are normalized to α-tubulin and expressed as fold-change relative to WT-CD. Data are presented as mean ± SEM (n = 7 per group). *P<0.05; **P<0.005.

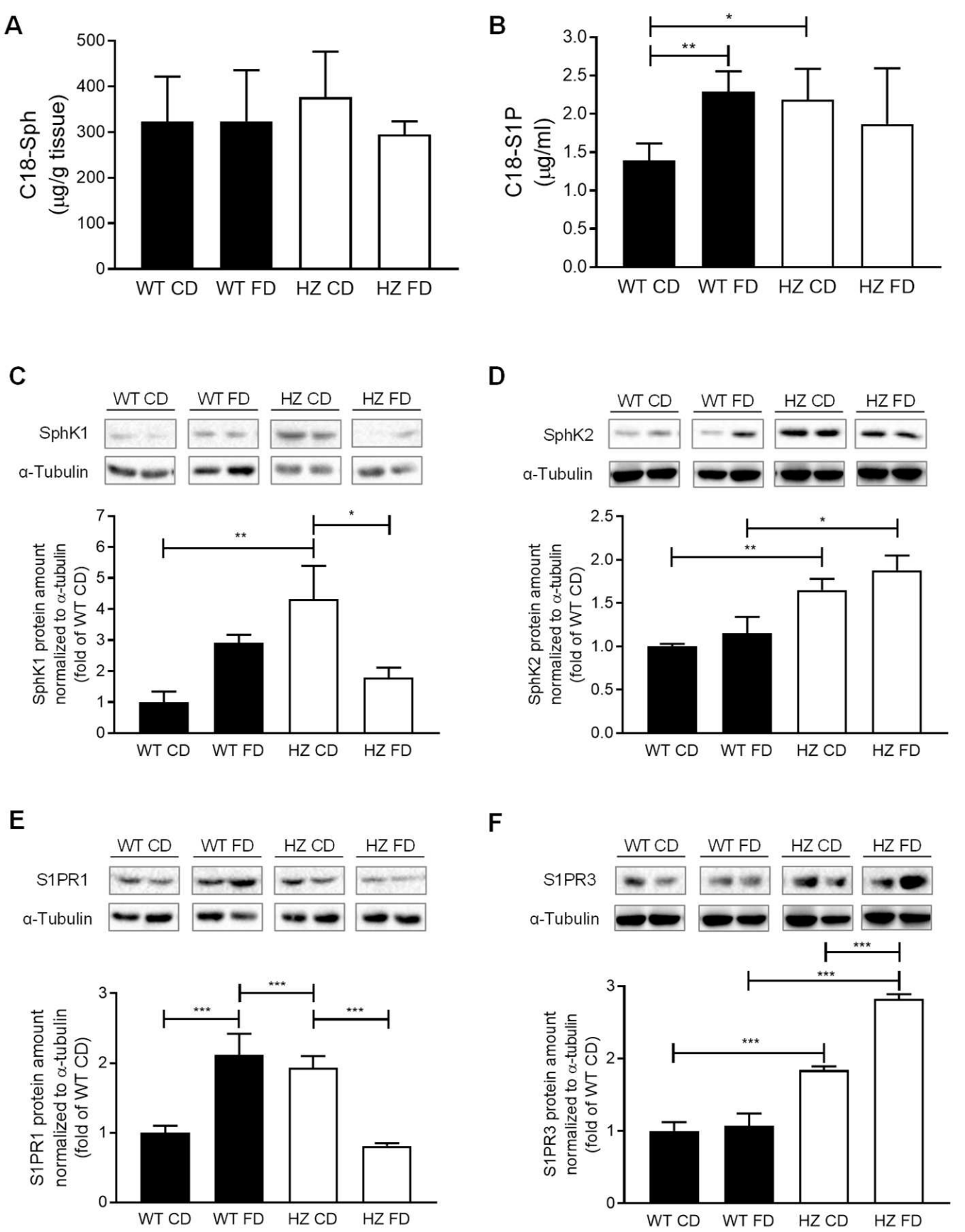
Figure 7. KRIT1 regulates lipid metabolism, S1P signaling, and inflammation in MEFs. Representative Western blots comparing KRIT1 knockout (K–/–) and KRIT1-reexpressing (K9/6) mouse embryonic fibroblasts (MEFs) for: (A) lipid and cholesterol biosynthesis markers (SREBP1c, SREBP2, HMG-CoA-R); (B) S1P production enzymes (SphK1, SphK2); (C) S1P receptors (S1PR1, S1PR3); and (D) inflammatory and fibrogenic proteins (TLR4, TGF-β, fibronectin). Data are representative of four independent experiments.

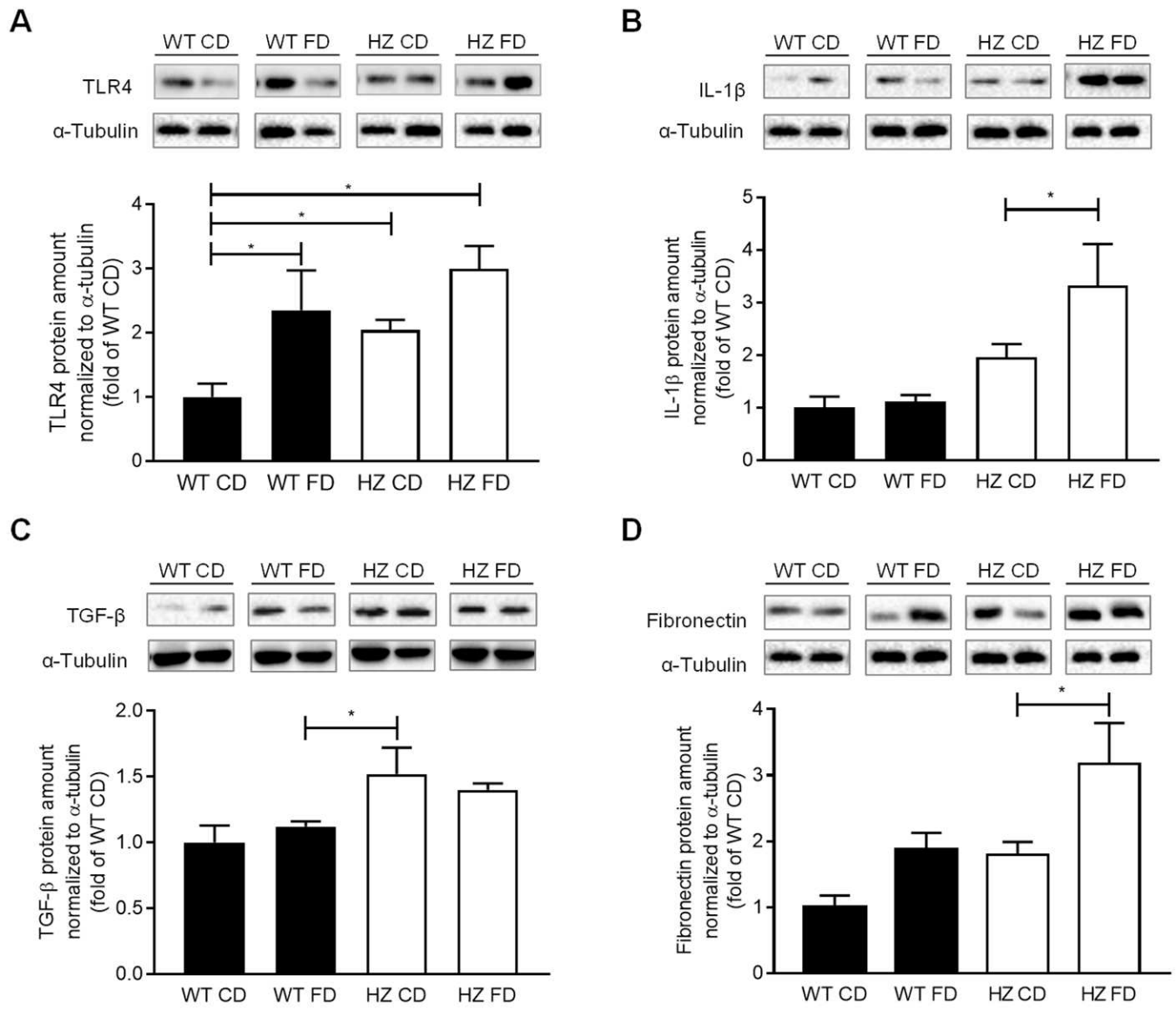

A
Pentosidine (ppb)
0
2
4
6
8
**
**
**
WT CD
WT FD
HZ CD
HZ FD
B
Carboxymethyl-lysine (ppb)
0
25
50
75
100
125
150
*
*
*
WT CD
WT FD
HZ CD
HZ FD
C
WT CD
WT FD
HZ CD
HZ FD
RAGE
α-Tubulin
RAGE protein amount normalized to α-tubulin (fold of WT CD)
0
1
2
3
4
5
***
**
**
WT CD
WT FD
HZ CD
HZ FD

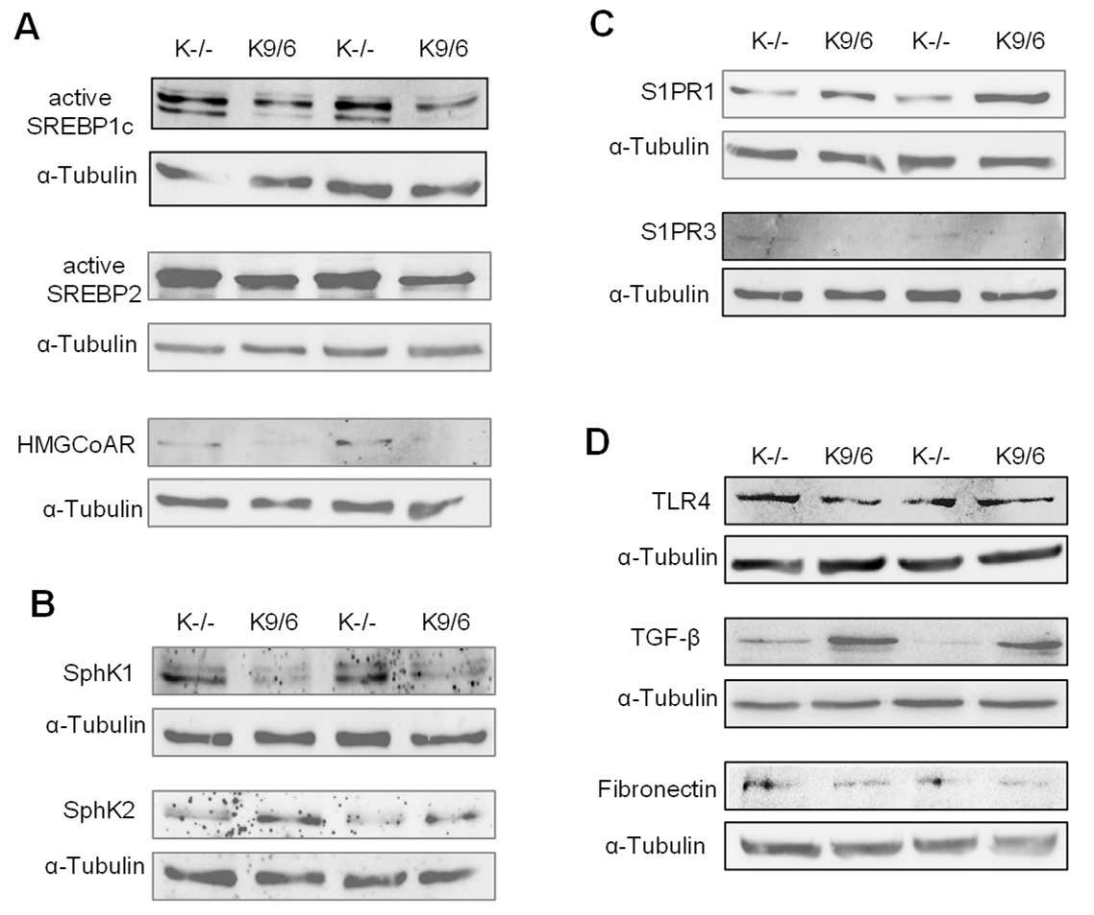

A
Plasma triglycerides (mg/dl)
100
80
60
40
20
0
WT CD
WT FD
HZ CD
HZ FD
B
Plasma total cholesterol (mg/dl)
140
120
100
80
60
40
20
0
*
WT CD
WT FD
HZ CD
HZ FD


A
WT CD
WT FD
HZ CD
HZ FD
Nuclear SREBP1c
PCNA
Nuclear SREBP1c protein amount normalized to PCNA (fold of WT CD)
3.0
2.5
2.0
1.5
1.0
0.5
0.0
*
*
*
WT CD
WT FD
HZ CD
HZ FD
B
Liver triglycerides (mg/dl)
400
300
200
100
0
**
*
WT CD
WT FD
HZ CD
HZ FD
C
WT CD
WT FD
HZ CD
HZ FD


A
WT CD
WT FD
HZ CD
HZ FD
Nuclear SREBP2
PCNA
Nuclear SREBP2 protein amount normalized to PCNA (fold of WT CD)
2.5
2.0
1.5
1.0
0.5
0.0
*
**
*
WT CD
WT FD
HZ CD
HZ FD
B
WT CD
WT FD
HZ CD
HZ FD
HMG-CoA-R
α-Tubulin
HMGCoA-R protein amount normalized to α-tubulin (fold of WT CD)
4
3
2
1
0
*
WT CD
WT FD
HZ CD
HZ FD
C
WT CD
WT FD
HZ CD
HZ FD
p-RhoA-Ser188
Total RhoA
p-RhoA/Total RhoA (fold of WT CD)
1.25
1.00
0.75
0.50
0.25
0.00
*
WT CD
WT FD
HZ CD
HZ FD
D
WT CD
WT FD
HZ CD
HZ FD
ROCK1
α-Tubulin
ROCK1 protein amount normalized to α-tubulin (fold of WT CD)
3
2
1
0
*
WT CD
WT FD
HZ CD
HZ FD
E
WT CD
WT FD
HZ CD
HZ FD
p-YAP-Ser127
Total YAP
pYAP/Total YAP (fold of WT CD)
1.5
1.0
0.5
0.0
**
*
WT CD
WT FD
HZ CD
HZ FD


A
C18-Sph (μg/g tissue)
500
400
300
200
100
0
WT CD
WT FD
HZ CD
HZ FD
B
C18-S1P (μg/ml)
3.0
2.5
2.0
1.5
1.0
0.5
0.0
*
**
WT CD
WT FD
HZ CD
HZ FD
C
WT CD
WT FD
HZ CD
HZ FD
SphK1
α-Tubulin
SphK1 protein amount normalized to α-tubulin (fold of WT CD)
7
6
5
4
3
2
1
0
**
*
WT CD
WT FD
HZ CD
HZ FD
D
WT CD
WT FD
HZ CD
HZ FD
SphK2
α-Tubulin
SphK2 protein amount normalized to α-tubulin (fold of WT CD)
2.5
2.0
1.5
1.0
0.5
0.0
*
**
WT CD
WT FD
HZ CD
HZ FD
E
WT CD
WT FD
HZ CD
HZ FD
S1PR1
α-Tubulin
S1PR1 protein amount normalized to α-tubulin (fold of WT CD)
3
2
1
0
***
***
***
WT CD
WT FD
HZ CD
HZ FD
F
WT CD
WT FD
HZ CD
HZ FD
S1PR3
α-Tubulin
S1PR3 protein amount normalized to α-tubulin (fold of WT CD)
3
2
1
0
***
***
***
WT CD
WT FD
HZ CD
HZ FD


A
WT CD
WT FD
HZ CD
HZ FD
TLR4
α-Tubulin
TLR4 protein amount normalized to α-tubulin (fold of WT CD)
0
1
2
3
4
*
*
*
WT CD
WT FD
HZ CD
HZ FD
B
WT CD
WT FD
HZ CD
HZ FD
IL-1β
α-Tubulin
IL-1β protein amount normalized to α-tubulin (fold of WT CD)
0
1
2
3
4
5
*
WT CD
WT FD
HZ CD
HZ FD
C
WT CD
WT FD
HZ CD
HZ FD
TGF-β
α-Tubulin
TGF-β protein amount normalized to α-tubulin (fold of WT CD)
0.0
0.5
1.0
1.5
2.0
*
WT CD
WT FD
HZ CD
HZ FD
D
WT CD
WT FD
HZ CD
HZ FD
Fibronectin
α-Tubulin
Fibronectin protein amount normalized to α-tubulin (fold of WT CD)
0
1
2
3
4
*
WT CD
WT FD
HZ CD
HZ FD


A
K-/-
K9/6
K-/-
K9/6
active SREBP1c
α-Tubulin
active SREBP2
α-Tubulin
HMGCoAR
α-Tubulin
B
K-/-
K9/6
K-/-
K9/6
SphK1
α-Tubulin
SphK2
α-Tubulin
C
K-/-
K9/6
K-/-
K9/6
S1PR1
α-Tubulin
S1PR3
α-Tubulin
D
K-/-
K9/6
K-/-
K9/6
TLR4
α-Tubulin
TGF-β
α-Tubulin
Fibronectin
α-Tubulin

Supplementary Files

This is a list of supplementary files associated with this preprint. Click to download.

- MastrocolaetalKeyMessages.docx
- MastrocolaetalOriginalBlots.pdf
- MastrocolaetSupplementaryMaterialsTableS1.docx